Right Handed or Left Handed? Forbidden X-Ray Diffraction Reveals Chirality

Yoshikazu Tanaka,[1] Tomoyuki Takeuchi,[1] Stephen W. Lovesey,[2] Kevin S. Knight,[3] Ashish Chainani,[1] Yasutaka Takata,[1] Masaki Oura,[1] Yasunori Senba,[4] Haruhiko Ohashi,[4] and Shik Shin[1]

[1]*RIKEN SPring-8 Center, Sayo, Hyogo 679-5148, Japan*

[2]*Diamond Light Source and ISIS Facility, Rutherford Appleton Laboratory, Oxfordshire, OX110QX, United Kingdom*

[3]*ISIS Facility, Rutherford Appleton Laboratory, Oxfordshire, OX110QX, United Kingdom*

[4]*Japan Synchrotron Radiation Research Institute (JASRI), Sayo, Hyogo 679-5198, Japan*

(Received 7 December 2007; revised manuscript received 24 February 2008; published 8 April 2008)

Enantiomers, or stereoisomers, have crystal structures that are mirror images of each other and are thus handed, like our right and left hands. The physical properties of enantiomers are identical except for optical activity, which rotates linearly polarized light by equal amounts but in opposite directions. While conventional x-ray Bragg diffraction can determine crystal structures, it does not distinguish between right- and left-handed crystals. We show resonant Bragg diffraction using circularly polarized x rays reveals the handedness of crystals by coupling x-ray helicity to a crystal screw axis. The intensity of resonantly allowed reflection of α-quartz is well described by an admixture of a parity-even and a parity-odd process. Our results are of general importance and demonstrate a new method to directly study chiral motifs in structures that include biomaterials, liquid crystals, magnets, multiferroics, etc.

DOI: 10.1103/PhysRevLett.100.145502 PACS numbers: 61.05.cp, 42.70.Ce, 61.05.cc

Handedness occurs in compounds ranging from amino acids, sugars, adrenaline to liquid crystals, as well as inorganic materials like tellurium and α-quartz (SiO_2). The structures of α-quartz crystals are described by one of the 11 enantiomorphic space-group pairs, namely, no. 152 ($P3_121$) for right quartz (R quartz) and no. 154 ($P3_221$) for left quartz (L quartz), and the atomic structures are illustrated in Fig. 1. This definition [1] of handedness accords with the crystallographic structure and differs from that determined by the optical activity. Unfortunately, the latter is generally used in the industrial world. Space groups in enantiomorphic pairs are characterized by the presence of a screw axis, or chiral axis, and these are labeled right-handed (3_1, 4_1, 6_1, 6_2) and left-handed (3_2, 4_3, 6_5, 6_4). The first observation of optical activity in quartz, a rotation of the orientation of linearly polarized light, was reported in 1811 by Arago [2]. However, conventional x-ray Bragg diffraction cannot differentiate between chiral pairs of right- and left-handed axes. This inherent limitation can be traced to the fact that the Thomson scattering amplitude is diagonal in the two-dimensional space of polarization states while the desired coupling arises from interference of diagonal and off-diagonal amplitudes. Resonant x-ray Bragg diffraction can overcome this limitation by tuning the primary energy to an atomic resonance, which may result in all four scattering amplitudes being different from zero. In this case, diffraction can sense the handedness of a screw axis when the primary radiation carries definite helicity, i.e., circular polarization. In very early work with unpolarized anomalous scattering, a breakdown of Friedel's rule and intensity differences for Bijvoet pairs of allowed reflections was used to differentiate between right- and left-handed crystals [3]. Here, using right- and left-circularly polarized (RCP and LCP) x-ray beams, we show the first evidence of resonant x-ray Bragg diffraction of a forbidden reflection successfully applied to study the chirality of quartz. The technique is more selective than optical activity, which is allowed in 15 crystal classes, four of which are not enantiomeric.

The resonant Bragg diffraction of forbidden reflections is known [4–6] to be derived from the polarization anisotropy of the x-ray susceptibility. Such reflections are referred to as ATS (anisotropy of the tensor of susceptibility) reflections and represent a *symmetry breaking* due to the anisotropy of charge densities at atomic sites on resonance. The anisotropy can be characterized by atomic tensors, or multipole moments, such as the magnetic dipole, electric quadrupole [7], magnetic octupole [8], anapoles [9], etc. The resonant technique has achieved significant impor-

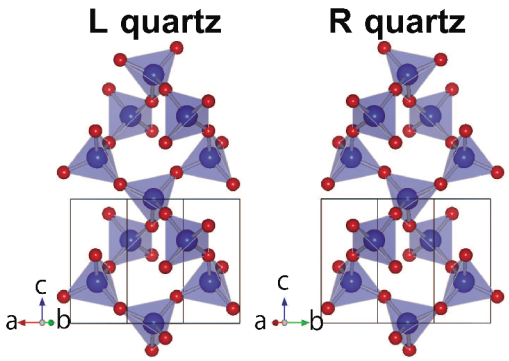

FIG. 1 (color). Views of atomic structure of R quartz (right) and L quartz (left) along the a^* axis and the b^* axis, respectively. The a^* and b^* axes are perpendicular to the plane of paper. Blue and red spheres represent Si and O atoms, respectively. Lines show the unit cell with hexagonal axes.

tance in the form of resonant soft x-ray scattering across $3d$ transition metal L-edges (such as Cu $2p$-$3d$ or Mn $2p$-$3d$) and has been successfully applied to study charge order in cuprates [10], orbital and magnetic order in manganites [11], etc. A recent review has detailed the progress in the field based on analyses for nonmagnetic and magnetic crystals [12]. In the present work, circularly polarized x-ray resonant diffraction, employing unique instrumentation available at the SPring-8 synchrotron facility, is used to define a new method to study chirality.

Experiments were carried out at beam line 17SU of the SPring-8 in Harima, Japan [13]. The incident energy was tuned in the vicinity of Si ($1s$) absorption edge. The spot size was about 20 μm in diameter. The circular polarization of the incident beam was switched by the electromagnet of the undulator [14]. The Stokes parameters [15], which represent the polarization of the x-ray beam are $P_2 = +0.95$ and $P_3 = -0.31$ for RCP and $P_2 = -0.95$ and $P_3 = -0.31$ for LCP beam, as obtained from the insertion device parameters of the beam line. The intensity of the diffracted beam was measured using a Si-photodiode sensor without polarization analysis. Samples were mechanically polished and mounted on the sample stage of the diffractometer which has two rotational axes for alignment. The azimuth axis Ψ ($-95° < \Psi < 95°$) enables us to measure the intensity as a function of the angle rotated about the scattering vector of the crystal. Here, the origin of the azimuth angle $\Psi = 0$ is defined by the reciprocal lattice vector a^* axis when the propagation vector $\mathbf{k}_i$ for incident beam and $\mathbf{k}_f$ for reflected beam have a relation that $\mathbf{k}_i \times \mathbf{k}_f$ is parallel to a^* and the sign + of Ψ is defined by the clockwise rotation about the scattering vector $\mathbf{k} = \mathbf{k}_f - \mathbf{k}_i$ as viewed looking up along the scattering vector.

Figure 2 shows the x-ray absorption spectrum (XAS) obtained in the total x-ray fluorescence yield mode and the integrated intensity of the space-group forbidden reflection 001 of L quartz as a function of the incident x-ray energy tuned across the Si ($1s$) absorption edge. For energies $\sim$10 eV below the absorption edge peak at 1847.93 eV, the diffraction peak intensity of 001 is negligible. On increasing the incident photon energy, the diffraction intensity undergoes a sharp maximum, followed by weaker features at higher energies. The most intense sharp peak in the 001 diffraction intensity corresponds to the highest intensity peak in the XAS.

We then used an incident beam of energy 1847.93 eV for measurements of reflection 001 as a function of azimuth angle Ψ. Figure 3 shows the result of azimuth angle scans performed on R quartz and L quartz with RCP and LCP incident beams, and we obtain a beautiful sinusoidal modulation exhibiting the threefold symmetry of the screw axis. Insets to Fig. 3 show the 2θ–θ scan profiles of reflection 001 observed at $\Psi = 0$. We note the following main features in data displayed in Fig. 3: (1) the integrated intensity of reflection 001 for R quartz for LCP (RCP) beam and that

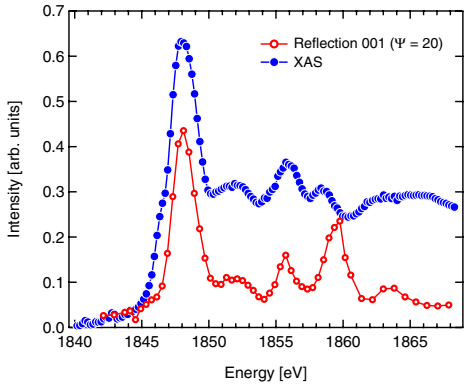

FIG. 2 (color online). XAS (filled circles) and integrated intensity (open circles) of reflection 001 of L quartz as a function of energy of the incident beam. Reflection 001 was measured at azimuth angle $\Psi = 20°$. The detection efficiency of the Si-photodiode is corrected for both curves but sample absorption is not corrected for the data of 001 reflection.

of L quartz for RCP (LCP) beam are comparable, and (2) the phase shifts of R quartz for both LCP and RCP, and, also, those of L quartz for both LCP and RCP, have the opposite sign with respect to the origin $\Psi = 0$. Thus, the diffracted intensities show evidence of a strong correlation between the helicity in the primary beam and the handedness of quartz.

In addition, we have measured reflection $00\bar{1}$ for L quartz. The measurements were performed on the back surface of the crystal used for reflection 001 measurements, obtained by a rotation of 180° about a^*. Figure 4 shows the result of azimuth angle scans for reflections 001

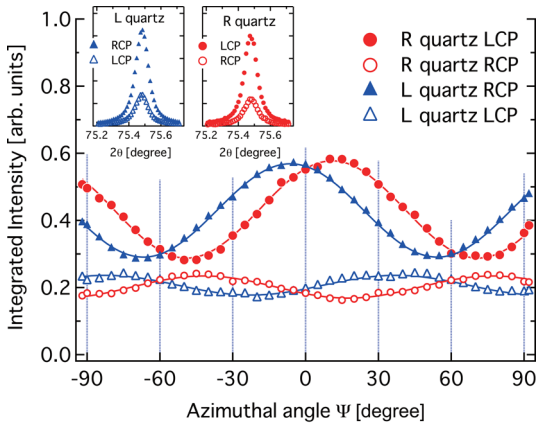

FIG. 3 (color online). Integrated intensity of reflection 001 of R and L quartz as a function of azimuth angle Ψ. Filled (open) circles represent the intensity of reflection 001 of R quartz measured with LCP (RCP) incident beam, and filled (open) triangles represent the intensity of reflection 001 of L quartz measured with RCP (LCP) incident beam. Each line shows a result of fit to data with functions expressed by Eq. (1) or (2). Inset shows the 2θ–θ scan profiles of reflection 001 observed at $\Psi = 0$.

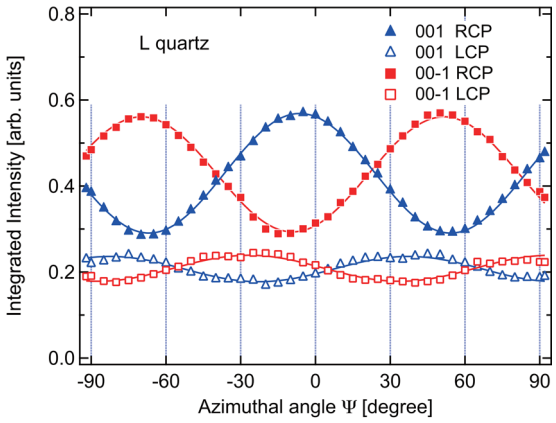

FIG. 4 (color online). Integrated intensity of reflection 001 and $00\bar{1}$ of L quartz as a function of azimuth angle Ψ. Measurements were done with RCP and LCP incident beam. Filled triangles (squares) represent the intensity of reflection 001 ($00\bar{1}$) measured with RCP incident beam, and open triangles (squares) represent the intensity of reflection 001 ($00\bar{1}$) measured with LCP incident beam. Each line shows a result of fit to data with functions expressed by Eq. (1) or (2).

and $00\bar{1}$ of L quartz. The results show that (1) the integrated intensity of reflections 001 and $00\bar{1}$ exhibit an antiphase relation with each other as a function of Ψ for the same helicity (a small discrepancy in antiphase is due to an artifact misalignment of the samples), (2) the integrated intensity for RCP x rays is higher than that for LCP x rays for both reflections 001 and $00\bar{1}$, and (3) the phase shift in azimuth angle Ψ is not the same for RCP and LCP beams. The observed antiphase behavior is anticipated as we shall see in the subsequent analysis.

The silicon site $(\bar{x}\,\bar{x}\,0)$ occurs in unit cells of both enantiomers of α-quartz and because of its commonality, it is used in calculations as the reference site. Right-handed orthonormal quantization axes $(\xi\,\eta\,\zeta)$ for the reference site have the ξ-axis coincident with the diad axis of symmetry through $(\bar{x}\,\bar{x}\,0)$ and the ζ-axis coincident with the crystal c axis. Evidently, physical properties of quartz are not changed by rotation of the crystal by 180° about the ξ-axis and, therefore, diffracted intensities at $00l$ and $00\bar{l}$ are the same. It is convenient in our presentation to label the enantiomers by an index $\nu = \pm 1$ that subsequently acquires physical significance as a label for crystal chirality. Space-group no. 152 is labeled $\nu = +1$ (right-handed screw 3_1) and space-group no. 154 is labeled $\nu = -1$ (left-handed screw 3_2). In a diffraction experiment the orientation of a crystal is most conveniently made by reference to reciprocal lattice vectors. For reflections $00l$ of interest, we shall measure a rotation by an angle Ψ about the Bragg wave vector $00l$ relative to a setting of the crystal with a^* perpendicular to the plane of scattering. The reciprocal lattice vector a^* is normal to the c axis, and a^* and the ξ axis enclose an angle of 30°. In consequence, intensities at $00l$ and $00\bar{l}$ as functions of Ψ are offset by $+30°$ and $-30°$, respectively, from $\Psi = 0$. Hence, the antiphase relation or 60° offset seen in Fig. 4 is due to a rotation of 180° about a^*. In other words, this is the property of point group D_3.

Our analysis of diffracted intensities respects all atomic and crystal symmetries. It is based on a resonant scattering amplitude, correct up to the order of the electric quadrupole event [12,16]. The amplitude is expressed in terms of unique structure factors for sites $3a$ (Wyckoff letter a and multiplicity 3) in space groups nos. 152 and 154. A structure factor is constructed in terms of atomic multipoles assigned to the available valence electron states, and both parity-even and parity-odd multipoles are allowed since sites $3a$ are not centers of inversion symmetry. Multipoles are defined with respect to quantization axes for our chosen reference site, and they respect the diad symmetry parallel to the ξ-axis. Multipoles for the two remaining sites in a unit cell are derived from the reference site by application of the elements of symmetry in the space group. Translational symmetry in a unit cell generates structure factors for reflections $00l$ with threefold periodicity and the sense of handedness is opposite for 3_1 and 3_2.

In the general case, the total amplitude for resonant diffraction is a coherent sum of amplitudes for various parity-even and parity-odd processes at resonance energies that need not to be the same. There are four amplitudes for the polarization channels in diffraction that are commonly labeled $\sigma'\sigma$, $\pi'\sigma$, $\pi'\pi$, and $\sigma'\pi$ where a prime denotes the secondary (diffracted) beam [12,16]. In the extreme case that the primary beam is fully π-polarized (linear in the plane of scattering, $P_3 = -1$), diffraction is confined to amplitudes $(\pi'\pi)$, and $(\sigma'\pi)$ and schematically the total diffracted intensity is $|(\pi'\pi)|^2 + |(\sigma'\pi)|^2$. For diffraction enhanced by a single, isolated resonance, this intensity is the same for space groups nos. 152 and 154 and thus independent of screw axes. For the present case of dominantly circular polarization, helicity in the primary beam, P_2, contributes an intensity $P_2\mathrm{Im}.\{(\sigma'\sigma)(\sigma'\pi)^* + (\pi'\sigma) \times (\pi'\pi)^*\}$ to the total intensity. For diffraction at $00l$, and an enhancement from an isolated resonance, the contribution to the intensity which is proportional to P_2 conveys a correlation between the x-ray helicity and the crystal chirality since it has opposite signs for the enantiomorphic screw-axes 3_1 and 3_2. In the Eqs. (1) and (2) stated below, the correlation in question leads to $I_j(\nu, P_2) = I_j(-\nu, -P_2)$ with $j = 0$ and 1. These identities are found to be exact for an isolated resonance and, also, for the more general case of two well-separated resonances of opposite parity that are necessary for a successful analysis of our measured intensities.

Intensity predicted from the $E1$-$E1$ ($E1$ represents the electric dipole) resonant process at 001 contains only even harmonics of 3Ψ whereas our data possesses both even and odd harmonics. However, such harmonics of 3Ψ are predicted by a coherent sum of resonant processes of opposite

(even and odd) parity, and intensities calculated for 001 or $00\bar{1}$ are given by

$$I_{\pm}(\nu = +1) = I_0(+, P_2) \pm I_1(+, P_2)\sin(3\Psi) - (\pm)I_2(+, P_2)\cos(3\Psi), \quad (1)$$

and,

$$I_{\pm}(\nu = -1) = I_0(-, P_2) - (\pm)I_1(-, P_2)\sin(3\Psi) \pm I_2(-, P_2)\cos(3\Psi). \quad (2)$$

The choice of origin for Ψ, a displacement of 30° away from our ξ-axis, converts even harmonics of 3Ψ to odd harmonics and vice versa, and, also, yields opposing signs of trigonometric functions at 001 and $00\bar{1}$. Dependence on helicity in the primary x-ray beam, $P_2 = +0.95$ or -0.95, is observed explicitly in our experiments. Other variables in $I_j(\nu, P_2)$ include atomic multipoles that describe ground-state properties of Si ions in quartz. Parity-odd multipoles are called polar multipoles, with the polar dipole represented by a unit position vector and the polar quadrupole is a product of angular momentum and an anapole operator [12].

The derived identity $I_2(+, P_2) = -I_2(-, -P_2)$ demonstrates a fundamental correlation between crystal chirality (ν) and helicity (P_2). A similar interpretation applies to our findings $I_0(+, P_2) = I_0(-, -P_2)$ and $I_1(+, P_2) = I_1(-, -P_2)$ for two resonances separated in energy by an amount that is large compared to resonance widths. Inspection of entries in Table I shows that these three relations for $I_j(\nu, P_2)$ are satisfied by our data, to a good approximation. In other words, screw operations enantiomorphically (mirror) related to each other (3_1 and 3_2 in α-quartz) correlate with the handedness of helicity (P_2), together with the handedness of rotation of the crystal and are explicitly accounted for in Eqs. (1) and (2).

Values of $I_j(\nu, P_2)$ inferred from our data have been checked not to be consistent with expressions derived from a sum of $E1$-$E1$ and $E1$-$M1$ processes ($M1$ represents the magnetic dipole). This finding is consistent with the expectation that these particular resonances are separated in energy by a small amount, while our data imply a large separation which is more likely the case if the parity-odd process $E1$-$E2$ ($E2$ represents the electric quadrupole) mixes with $E1$-$E1$ in the scattering amplitude. A mixture of two parity-even processes, e.g., $E1$-$E1$ and $E2$-$E2$, also does not produce the identity $I_2(+, P_2) = -I_2(-, -P_2)$ that is so well supported by our data.

Our findings demonstrate that, circularly polarized x rays detect the chirality of quartz through an admixture of $E1$-$E1$ and $E1$-$E2$ resonant processes which is visible at space-group forbidden reflections 001 or $00\bar{1}$, because of angular anisotropy in Si parity-even and parity-odd atomic multipoles. The technique is generally applicable to chiral motifs and while studies on liquid crystals using resonant x-ray diffraction have succeeded in characterizing specific incommensurate and helicoidal structure models [17,18], a direct measurement of the handedness of chirality in liquid crystals is still elusive. We envisage direct applications for measuring the handedness of chirality using resonant x-ray diffraction of forbidden reflections at specific x-ray absorption edges of biomolecules, liquid crystals, ferro- and antiferroelectrics, multiferroics, etc.

TABLE I. Inferred values of $I_j(\nu, P_2)$, which appear in Eqs. (1) and (2), for $\nu = \pm 1$ and $P_2 = \pm 0.95$. Each value has the standard deviation about 0.01 to 0.02.

		$P_2 = 0.95$ (RCP)			$P_2 = -0.95$ (LCP)		
	ν	I_0	I_1	I_2	I_0	I_1	I_2
R quartz 001	+1	2.01	−0.26	0.20	4.32	0.77	−1.21
L quartz 001	−1	4.20	0.44	1.31	2.06	−0.27	−0.10
L quartz $00\bar{1}$	−1	4.27	0.60	1.19	2.09	−0.30	−0.05

We thank K. Shirasawa, T. Tanaka, M. Takeuchi, Y. Furukawa, T. Hirono, T. Ohata, H. Kitamura, and T. Ishikawa for valuable support, and for the construction and commissioning of beam line 17SU of the SPring-8.

[1] A. M. Glazer and K. Stadnikca, J. Appl. Crystallogr. **19**, 108 (1986).
[2] F. Arago, Mem. Cl. Sci. Math. Phys. Inst. **12**, 93 (1811).
[3] J. M. Bijvoet, Nature (London) **173**, 888 (1954).
[4] D. H. Templeton and L. K. Templeton, Acta Crystallogr. Sect. A **36**, 237 (1980).
[5] V. E. Dmitrienko, Acta Crystallogr. Sect. A **39**, 29 (1983).
[6] K. D. Finkelstein, Q. Shen, and S. Shastri, Phys. Rev. Lett. **69**, 1612 (1992).
[7] Y. Tanaka *et al.*, Phys. Rev. B **69**, 024417 (2004).
[8] D. Mannix, Y. Tanaka, D. Carbone, N. Bernhoeft, and S. Kunii, Phys. Rev. Lett. **95**, 117206 (2005).
[9] S. W. Lovesey, J. Fernández-Rodríguez, J. A. Blanco, D. S. Sivia, K. S. Knight, and L. Pao- lasini, Phys. Rev. B **75**, 014409 (2007).
[10] P. Abbamonte, A. Rusydi, S. Smadici, G. D. Gu, G. A. Sawatzky, and D. L. Feng, Nature Phys. **1**, 155 (2005).
[11] K. J. Thomas *et al.*, Phys. Rev. Lett. **92**, 237204 (2004).
[12] S. W. Lovesey, E. Balcar, K. S. Knight, and J. Fernández-Rodríguez, Phys. Rep. **411**, 233 (2005).
[13] H. Ohashi *et al.*, AIP Conf. Proc. **879**, 523 (2007).
[14] K. Shirasawa, A. Hiraya, T. Tanaka, and H. Kitamura, Phys. Rev. ST Accel. Beams **7**, 020702 (2004).
[15] L. D. Landau and E. M. Lifshitz, *Quantum Electrodynamics* (Pergamon, Oxford, 1982), Vol. 4, 2nd ed.
[16] S. P. Collins, S. W. Lovesey, and E. Balcar, J. Phys. Condens. Matter **19**, 213201 (2007).
[17] P. Mach, R. Pindak, A.-M. Levelut, P. Barois, H. T. Nguyen, C. C. Huang, and L. Furenlid, Phys. Rev. Lett. **81**, 1015 (1998).
[18] L. S. Hirst *et al.*, Phys. Rev. E **65**, 041705 (2002).